Tikrit Journal of Pure Science Vol. 31 (3) 2026

DOI:https://doi.org/10.25130/tjps.v31i3.2126

IRAQI Academic Scientific Journals

Tikrit Journal of Pure Science

ISSN: 1813 – 1662 (Print) --- E-ISSN: 2415 – 1726 (Online)

Journal Homepage: https://tjpsj.org/

Tikrit Journal of Pure Science

Structural Model for the Northwestern Plunge of Safeen Anticline, Northeastern Iraq

Israa Thamar Dali[1], Abdulkhaleq A. Alhadithi[2]

[1,2]Department of Applied Geology, College of Science, University of Anbar-Iraq

Received: 21 Dec. 2025 **Received in revised forum:** 18 Apr. 2026 **Accepted:** 24 Apr. 2026

Final Proofreading: 12 May. 2026 **Available online:** 25 Jun. 2026

ABSTRACT

The northwest-southeast trending Safeen Anticline is located within the high folded zone of the Zagros fold and thrust belt within the Foreland. Ten stations were selected through an approximately north-south traverse. Different types of tension joints, shear fractures and faults, as well as their relationships, were studied, showing the influence of pre-existing normal faults and indicating at least two phases of compressional stress separated by a relaxation phase. Each compressional phase influenced the structural model. The second phase was a thrust that affected the southwestern limb and was accompanied by synchronous strike-slip movement with a trend of 029 °. The second was a back thrust that affected the northeastern limb at different time periods, with a trend of 020 ° for Б1. A second phase of relaxation occurred after the back thrust. Previous studies have confirmed the variation in the vergence between the Foreland folds, but this study confirms why the vergence varies within the individual traverse.

Keywords: Back-thrust, Safeen anticline, Shear fracture, Strike-slip fault, Tension joints, Thrust, Vergence.

Name: Israa Thamar Dali **E-mail:** esr23s4003@uoanbar.edu.iq

Tikrit Journal of Pure Science Vol. 31 (3) 2026
DOI:https://doi.org/10.25130/tjps.v31i3.2126

الموديل التركيبي للجزء الشمالي الغربي من طية سفين المحدبة، شمال شرق العراق

اسراء ثامر دلي[1]، عبد الخالق عبد الملك الحديثي[2]
[2,1] قسم الجيولوجيا التطبيقية، كلية العلوم، جامعة الانبار، الرمادي، العراق

الملخص

تقع طية سفين المحدبة ذات الاتجاه الشمالي الغربي–الجنوبي الشرقي ضمن منطقة الطيات العالية لحزام طي وتصدع زاغروس، التي تمثل الحافة الشمالية الشرقية للصفيحة العربية. تم اختيار عشر محطات من خلال مسار شمال–الجنوب تقريبا. أظهرت دراسة انواع مختلفة من فواصل الشد، وكسور القص، وأنواع الصدوع المختلفة، والعلاقة بين هذه الكسور، تأثير الصدوع الطبيعية الموجودة مسبقًا، وأن هناك مرحلتين على الأقل من إجهادات الضغط تفصل بينهما مرحلة استرخاء. أثرت كل مرحلة من مراحل الضغط على الموديل التركيبي بصورة مختلف عن المرحلة الاخرى، مثلت الأولى مرحلة دفع أثرت على الجناح الجنوبي الغربي التي رافقها حركة مضربيه متزامنة، خلالها كان اتجاه محور الاجهاد الرئيسي 29° والثانية مرحلة الدفع المعاكس التي أثرت على الجناح الشمالي الشرقي على التوالي، وفي فترات زمنية مختلفة خلالها كان اتجاه محور الاجهاد الرئيسي 20°. أكدت الدراسات السابقة التباين في الاتكاء بين طيات الفورلاند، لكن هذه الدراسة أكدت سبب اختلاف الاتكاء ضمن المسار نفسه.

INTRODUCTION

The northwestern part of the Safeen Anticline, which is concerned, is located between the latitudes (36° 26' 13") N and (36° 24' 49") N and longitudes (44° 15' 33") E and (44° 17' 58") E. Figure 1. Previous studies have shown that rock fractures or brittle deformations are closely related to a region's tectonic history [1-5]. The direction of the maximum principal stress and the counterclockwise rotation of the Arabian Plate led to fractures forming along the main directions in northeastern Iraq. [6-13]. There are four tectonic phases across the northeastern part of Iraqi territory; two of them are compressional. At the same time, the other.

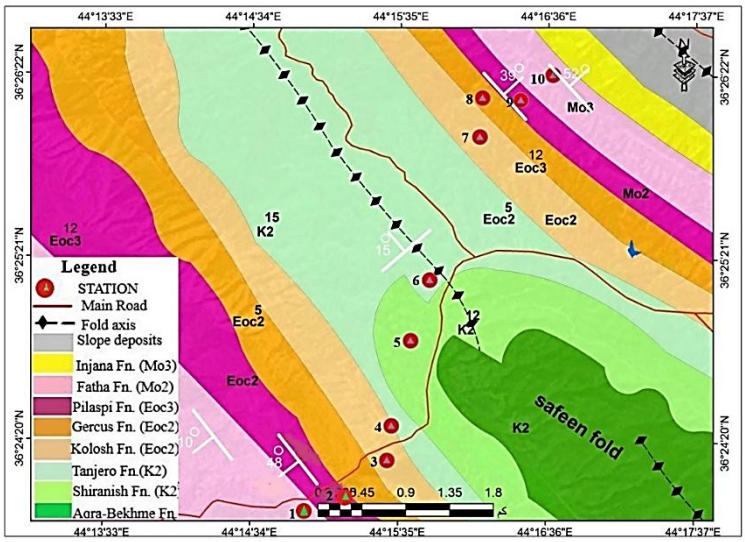

Fig. 1: Geological map of the study area (modified from 16).

phases are extensive, both phases are perpendicular to fold axes in the NE–SW direction or parallel to the NW–SE direction[14]. These stresses have caused the fold vergences in northwestern Iraq to be either towards the northeast or the southwest [12, 15]. Stratigraphy: seven formations are exposed along

the chosen traverse. The oldest is the Shiranish Formation (Early Maastrichtian), which is exposed in the core of the fold within the plunging area and consists of three lithostratigraphic units characterized by limestone, marl, and shale, with variable thicknesses. The unconformably overlying the Bekhme Formation is conformably overlain by the Tanjero Formation in the study area [16]. The Tanjero Formation (Late Cretaceous) consists of a succession of marly limestone and marl; this alternation of hard and soft rocks produces intense fractures and local fault-related folds (2, left). Kolosh Formation (Paleocene) consists of soft black rocks, sand, silt and clay [17]. The Khurmala Formation (Early Eocene) is found as a tongue within the upper part of the Kolosh Formation, which consists mainly of fossiliferous limestones that are white to light brown, well-bedded, massive, fractured, dolomitic and bituminous (figure 2, right). The Gercus Formation (Eocene) consists of a stratified succession of red mudstone and siltstone, with limited sandstone [17]. Pilaspi Formation (Upper Eocene) consists of white and gray limestone and dolostone. There is a bed of conglomerate between the Gercus and Pilaspi formations. The youngest Fatha Formation (Middle Miocene) consists of thick reddish-brown mudstone, interbedded with thin layers of limestone and gypsum Figure 1. It was mentioned above that the Foreland folds have variable vergence, but field observations indicate that the vergence of the Safeen Anticline changes within the given traverse; hence, the importance of the study is that the vergence varies within a single traverse. The study aims to provide an accurate interpretation of the tectonic history of the study area by examining fracture types, the effects of faults on the structural model of the fold, and the reasons for the variation in vergence along the given traverse.

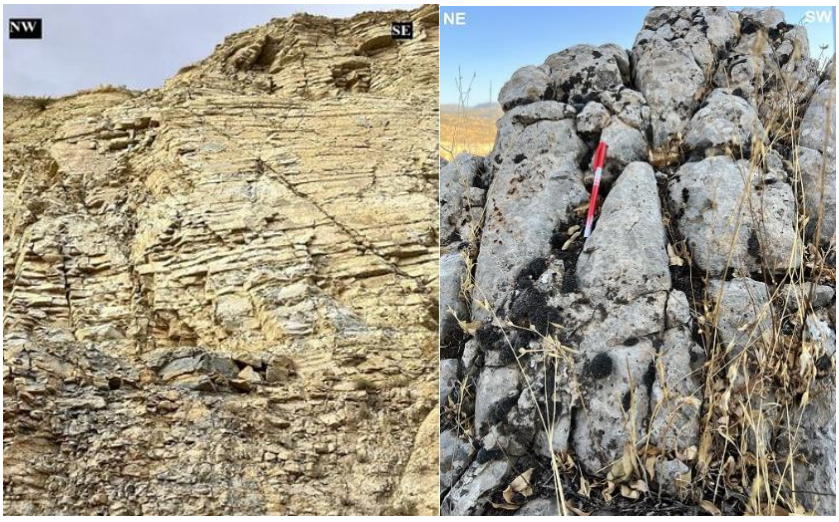

Fig. 2: (left) Intense fracture and thin layers of marly limestone bedded with thinner layers of marl, Shiranish Formation, (right) Khurmala Formation within Kolosh Formation.

MATERIALS AND METHODS

The fieldwork was conducted in two stages: the first period lasted 7 days (18-24 October 2024), and the second visit lasted 4 days (13-16 February 2025) to complete the surveying. Checking some geological features, including attitudes, photos and recording data, it was necessary to collect data in the field by measuring the attitudes of the bedding planes and the fracture surfaces through locations of the exposed rocks, which includes determining (dip direction/ dip amount). The collected data comprise the attitudes of bedding planes, including strike, dip, and dip direction, as well as the trend, plunge, and rake of slickensides or slickens lines, when necessary. In addition, fault types were identified and verified using Google Earth imagery. The attitude measurements were obtained using a Silva compass, following the Right-Hand Rule

(R.H.R.R.) convention for consistent data recording and stereographic representation. Some geological software was employed for data analysis, including FaultKinWin 7.5 (2016), developed by Richard W and stereo-net versions 11.6.1 - 2024. Allmendinger. This software was used to perform paleostress analysis based on fault-slip data. It plots the fault planes and their striations and determines the orientations of the principal stress axes (σ_1, σ_2, and σ_3).

RESULTS AND DISCUSSION

The fractures within the formations containing relatively solid rocks referred to above, the Shiranish, Pilaspi and Fatha formations, were measured and shown below.

Joints

The directions of the principal stress axes forming joints and their relationships were determined in figures (3, 4, 5, 6 and 7) and Table (1), which were compared with the directions of the stresses forming the faults. Joints are classified by origin and categorized as tension or shear joints. Also classified geometrically based on the three tectonic axes, a, b and c (1), joints are classified as groups when the joint surface contains two tectonic axes and the third is perpendicular to them and as systems when the joint surface intersects two tectonic axes and the third is parallel to them. [18].

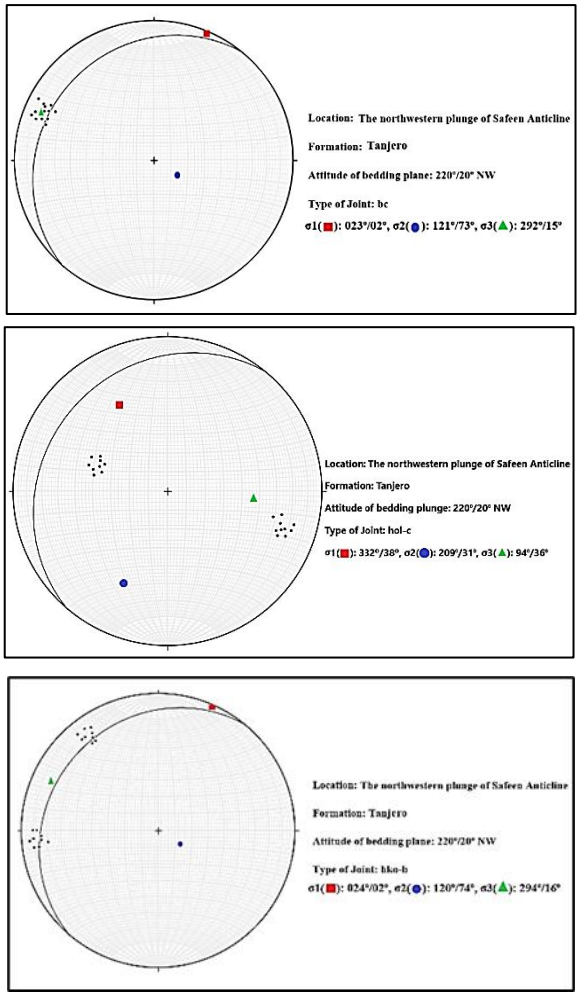

Fig. 3: Fractures within Tanjero Formation.

The most important and intense joints within the rocks of Shiranish Formation, located through the plunge area, which have a strike of 220°, are the hko-b joints, in which the attitude of the maximum principal stress axis (б1) is 024°/02°, the intermediate principal stress axis (б2) is 120°/74°.

DOI:https://doi.org/10.25130/tjps.v31i3.2126

The minimum principal stress axis (б3) is 294°/16°. They are consistent with the direction of the principal stress axes of the bc joints within the same layers that are almost parallel to the main compressive stress axes, which affect the northwestern area of the Safeen Anticline.

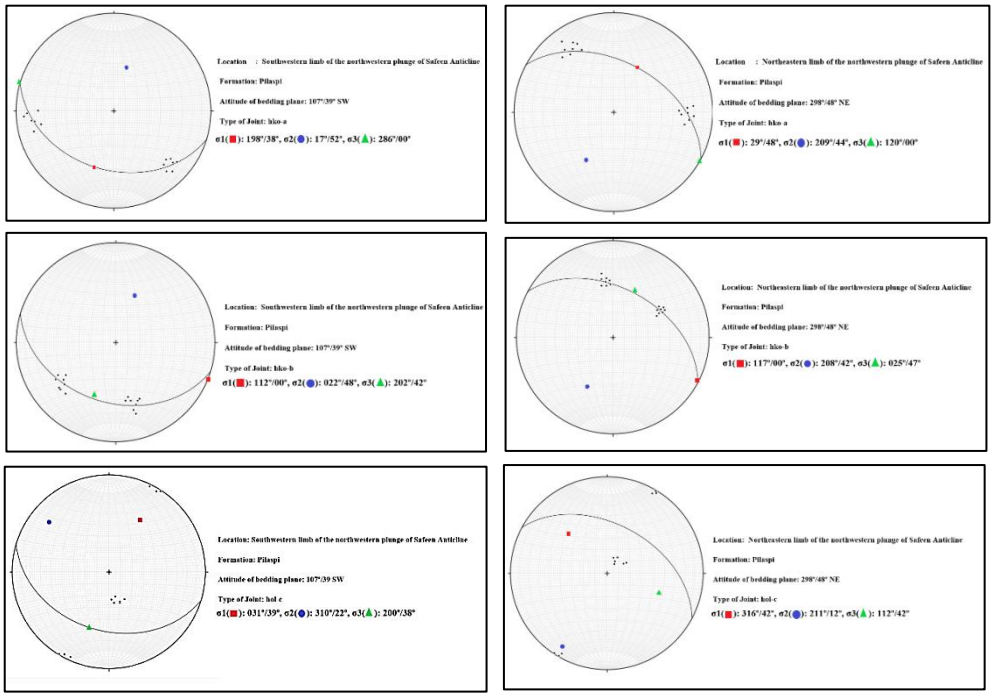

Fig. 4: Shear fractures within Pilaspi Formation.

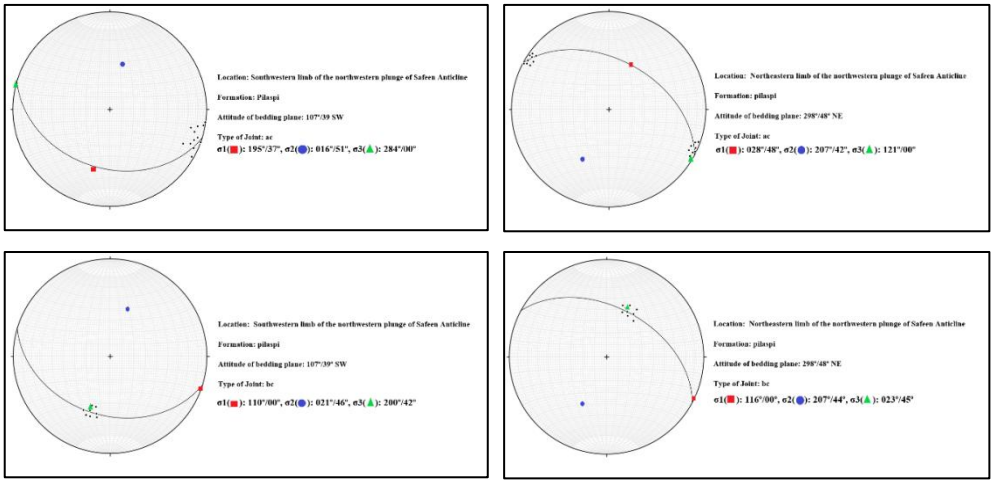

Fig. 5: Tension joints within Pilaspi Formation.

Tikrit Journal of Pure Science Vol. 31 (3) 2026

DOI:https://doi.org/10.25130/tjps.v31i3.2126

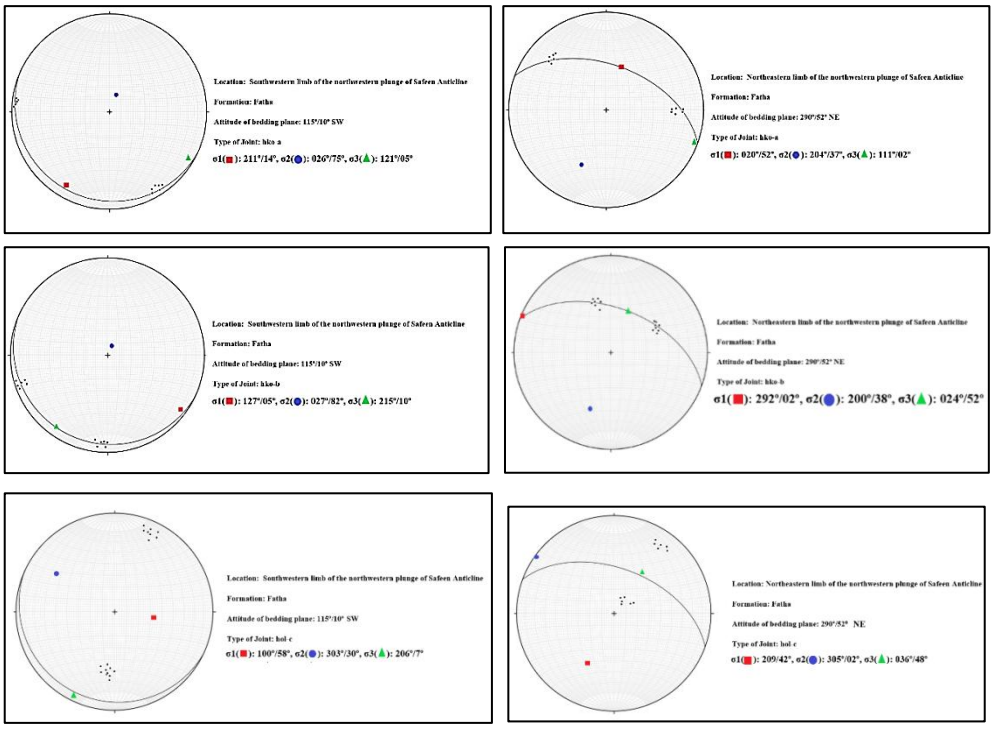

Fig. 6: Shear fractures within the Fatha Formation.

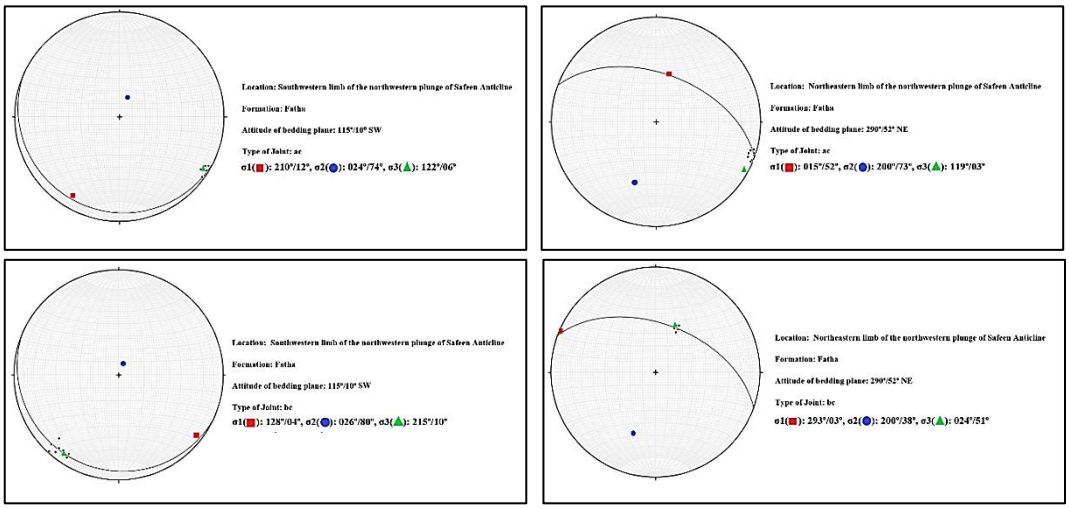

Fig. 7: Tension joints within the Fatha Formation.

Table 1: Principal stress axes and joint type

Formation and joint types	σ_1 (Trend/Plunge)	σ_2 (Trend/Plunge)	σ_3 (Trend/Plunge)
Tanjero – hko-b	024°/02°	120°/74°	294°/16°
Tanjero – hol-c	332°/38°	209°/31°	094°/36°
Tanjero – bc	023°/02°	121°/73°	292°/15°
Pilaspi – hko-a	198°/38°	017°/52°	286°/00°
Pilaspi – hko-a	029°/48°	209°/44°	120°/00°
Pilaspi – hko-b	112°/00°	022°/48°	202°/42°
Pilaspi – hko-b	117º/00º	208º/42º	025º/47º
Pilaspi – hol-c	031°/39°	310°/22°	200°/38°
Pilaspi – hol-c	316°/42°	211°/12°	112°/42°
Pilaspi – ac	195°/37°	016°/51°	284°/00°
Pilaspi – ac	028°/48°	207°/42°	121°/00°
Pilaspi – bc	110°/00°	021°/46°	200°/42°
Pilaspi – bc	116°/00°	207°/44°	023°/45°
Fatha – hko-a	211°/14°	026°/75°	121°/05°
Fatha – hko-a	020°/52°	204°/37°	111°/02°
Fatha – hko-b	127°/05°	027°/82°	215°/10°
Fatha – hko-b	292°/02°	200°/38°	024°/52º
Fatha – hol-c	100°/58°	303°/30°	206°/07°
Fatha – hol-c	209°/42°	305°/02°	036°/48°
Fatha – ac	210°/12°	024°/74°	122°/06°
Fatha – ac	015°/52°	200°/73°	119°/03°
Fatha – bc	128°/04°	026°/80°	215°/10°
Fatha – bc	293°/03°	200°/38°	024°/51°

Tension and shear joints are found within the layers of the Pilaspi Formation. The trend of б1 was taken into consideration, that compared with the trends of б1 for other types of joints and faults, the plunge of which will change with rotation or increasing dip of the rock layers, for example, the maximum principal stress axis forming joint systems (hko-a) that was horizontal at the beginning of the folding stage, when the rock layers are almost horizontal, however as the dip of the rock layers increases with continuous compressive stress, the plunge of the (б1) will increase. The trend of the (б1) forming the joints (hko-a) within the Pilaspi Formation layers of the northeast and southwest fold limbs is 029° and 198°, respectively, as shown in Figure 4. The trend of the (б1) forming the ac tension joints is 028° and 195° for the same limbs within the same rocks, respectively (figure 5), which corresponds to the trend of the stresses forming the shear fracture (hko-a).

The trend of the (б1) forming shear fracture systems (hko-a) in the Fatha Formation layers of the northeast and southwest limbs is 020° and 211°, respectively, as shown in Figure 6. The trend of the (б1) forming ac tension joints 015° and 210° of the northeast and southwest limbs, respectively, is shown in Figure 7. It is noted that the trend of the (б1) forming shear fractures and tension joints within the Fatha Formation layers is almost similar. Another important note is that the principal stress axes in the layers of the Pilaspi Formation differ from those in the Fatha Formation, indicating the presence of two distinct compressive stress stages. The first is called the thrust stage, and the second is the backthrust stage, as will be explained later in the faults. These two stages are separated by a

relaxation stage, represented by the attitudes of the principal stress axes of the shear fracture systems (hko-b) and the tension joint group (bc) within the rocks of the Pilaspi Formation (figures 4 and 5). This attitude of the principal stress axes differs from that of the rocks of the Fatha and Injana Formations figures (4-7). This is evidence of a second relaxation stage that followed the second compressive stage.

Faults

The three main types of faults: strike-slip, thrust and normal faults appeared, as will be mentioned later. These faults provided a clear interpretation of the tectonic history of the area and the structural model of the fold. Angular unconformity between the Tertiary formations indicates that folding occurred under the same field stress. Still, there is a noticeable change in the principal stress axes during different stages of stress, with the exchange of major tectonic stress axes leading to the development of different types of fractures. A major NNE-SSW right strike-slip fault was identified in figures (8 and 9), in addition to the thrust and back thrust faults in figures (10 and 11). These major faults played a significant role in the structural model of the fold's northwestern plunge. Field observations show two active phases during the Tertiary period. The first phase occurred after the deposition of the Pilaspi Formation (Late Eocene) by thrust may as a positive inversion fault along pre-existing listric fault that effect on Pilaspi Formation in the southwest limb, that causes the rocks of the formation dip steeper than the formation rock in the northeast limb figure (11 and 12) most of the thrusts or detachments in northeastern Iraq, resulting from the collision of the Arabian and Eurasian plates, occurred along extensional fault surfaces formed when the northeastern margin of the Arabian Plate followed a passive margin. [6-8]. Not only variations in dip between two limbs but also within the same limb, the right-lateral strike movement through the southwest limb, in which the northwestern block dips steeper than the southeastern block. The second phase occurred after the deposition of the Fatha Formation (Middle Miocene), during which a backthrust affected the Fatha Formation rocks in the northeast limb (figures 11 and 12).

Fig. 8: strike-slip fault (Transversal fault) in the southwestern limb within the northwest plunge of the Safeen Anticline. Note that the plunge of the Pilaspi Formation layers in the northwest block has rotated clockwise toward the southeast, not toward the northwest, due to dextral movement.

The right-lateral strike-slip fault within the study area may have formed. Synchronized with compressive stresses, the most important indicator of this is the different inclination of the layers on both sides of the strike-slip fault. The dip of the Pilaspi rocks in the northwest block of the strike-slip fault in the southwest limb is 59°, while the corresponding dipping of the same rocks in the southeast block within the same limb is 45°. The second piece of evidence for strike-slip movement is that the structures, e.g., fault-propagation folds, within the northwest block differ from those in the

southeast block. Another evidence of the strike-slip movement is the northwestward plunge of the Safeen Anticline along the traverse, which was towards the southeast, not towards the northwest, as a result of the clockwise rotation of the Pilaspi layers in the northwestern block of the southwest limb (figures 8 and 10).

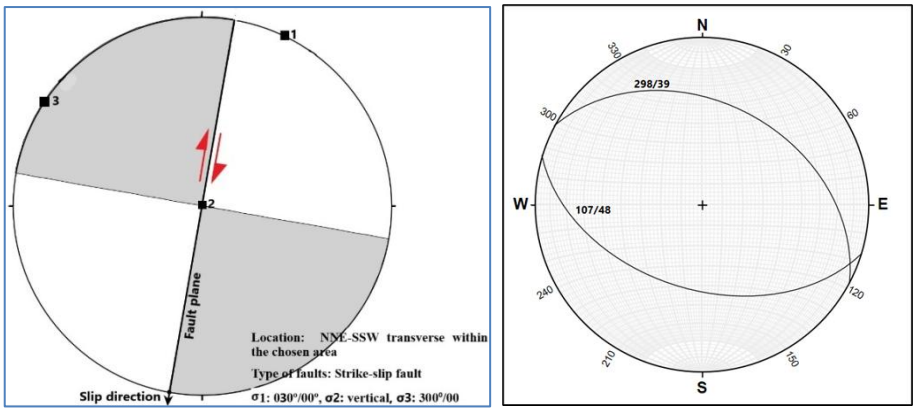

Fig. 9: Fault plane shows dextral fault with principal stress axes (left). Attitude of the Pilaspi Formation within the area that is affected by strike-slip movement (right), plunge of the anticline toward NW except along the dextral fault, the plunge is toward SE due to the rotation of the beds by strike movement (see Fig. 8).

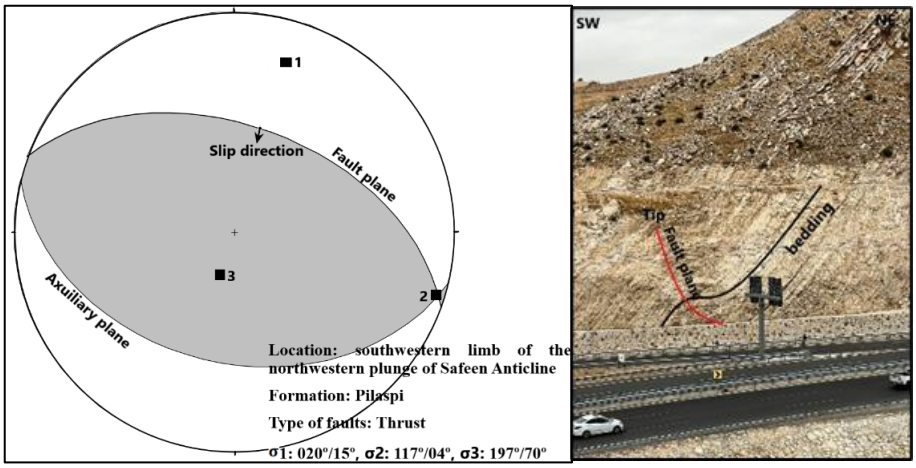

Fig. 10: Fault plane shows fault trace within Pilaspi Formation (left), the image showing the fault-propagation fold due to thrust in the northwestern block of the strike-slip fault (right).

Tikrit Journal of Pure Science Vol. 31 (3) 2026
DOI:https://doi.org/10.25130/tjps.v31i3.2126

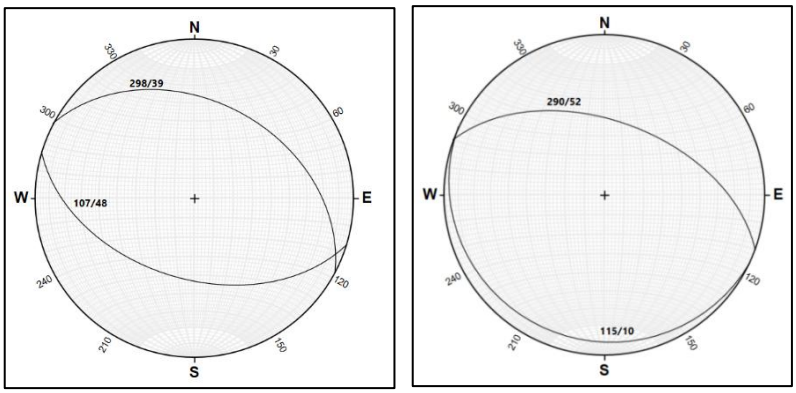

Fig. 11: Stereographic projection of the northwestern plunge of Safeen Anticline (left) through the beds of Pilaspi Formation, with a steep dip of the SW limb due to thrusting. (right) through the beds of the Fatha Formation, a steep dip of the NE limb due to backthrust.

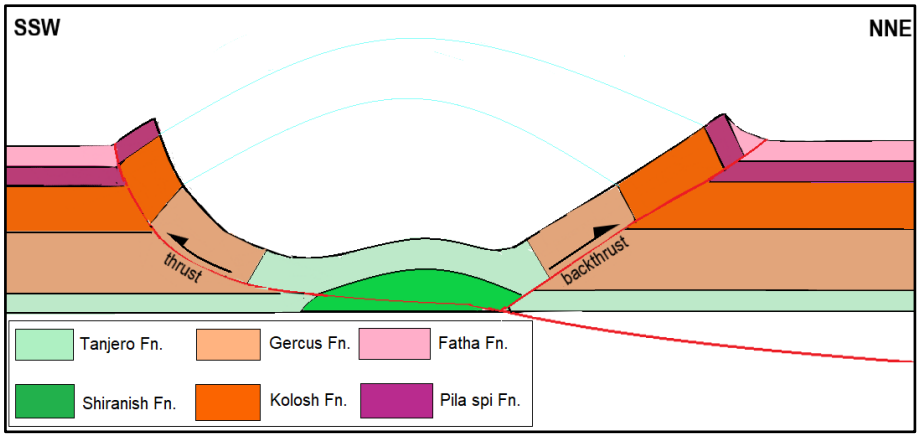

Fig. 12: Structural model of the northwestern plunge of Safeen Anticline along a dextral fault.

Another thrust fault appeared within the rocks of the Shiranish Formation at the plunge of the fold; it has the same attitude of strike, dip and dip direction, indicating that the fault that affected the Tanjero rocks is a splay fault, which makes the fault area higher than its surroundings (figure 13). The thrust fault accompanies the piggy-back phenomenon. Initially, fault no. 1 formed; after reactivation of the main fault, fault no. 2 formed, increasing the dip of fault no. 1; after further reactivation, fault no. 3 formed, which in turn increased the dip of the previous two faults. Positive flower structure accompanied fault no. 1 figure (14).

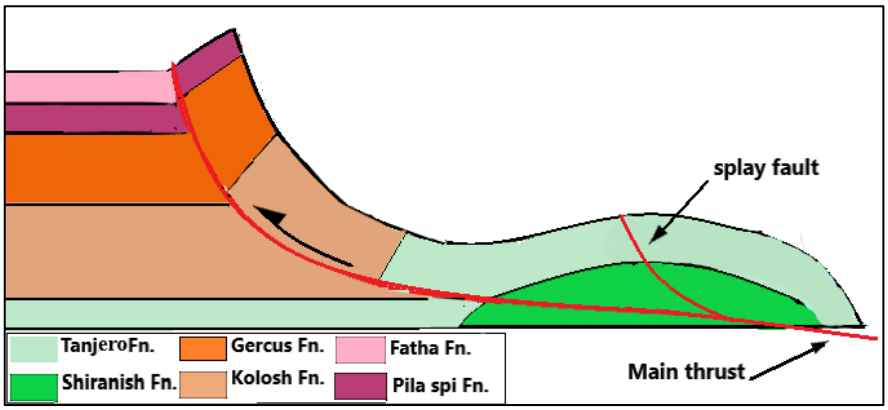

Fig. 13: The main fault affected the rocks of the Pilaspi Formation, while the splay fault affected the rocks of the Tanjero Formation.

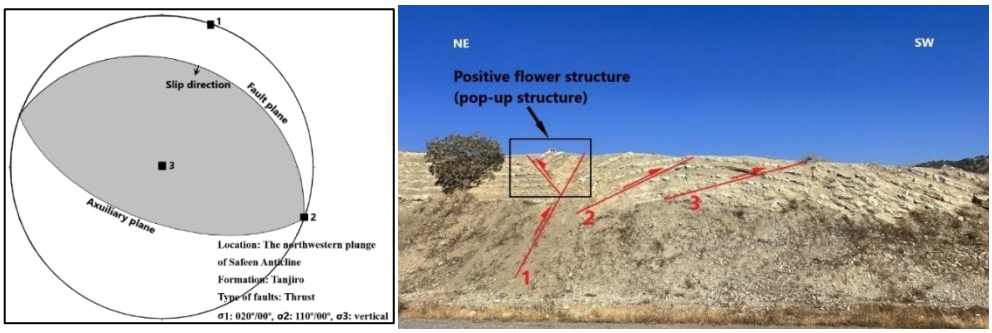

Fig. 14: fault plane shows a thrust fault in the Tanjero Formation (left). The piggy-back phenomenon is accompanied by the fault (right).

The third type of fault is a normal fault. There is a major normal fault located within the rocks of the Shiranish Formation, extending for a relatively long distance in a northwest-southeast direction (figure 15). The trend of the maximum principal stress axis is 035°/64°, the intermediate stress axis is 298°/03°, and the minimum stress axis is 207°/24°, in addition to local normal faults affecting the thin limestone layers of the Avanah Formation, which appear as lenses within the Gercus Formation, with other local normal faults within the Fatha Formation in the northeastern limb due to the second relaxation.

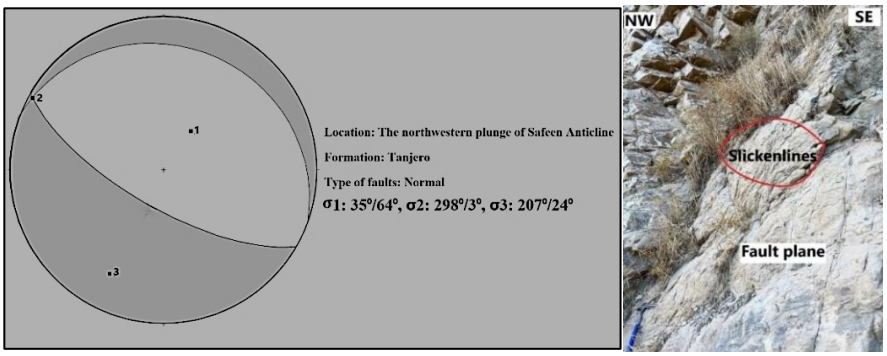

Fig. 15: Fault plane shows normal faults in the Shiranish Formation (left). Photo of the fault (right)

CONCLUSION

The stereographic projection of the measured fracture poles within the Pilaspi and Fatha formations showed that the NE-SW stresses formed the shear fractures hko-a, and the tension joints ac have the same trend and were formed during the first stage of compressive stresses. The NW-SE stresses that formed the shear fractures hko-b have the same trend as the stresses forming the tension joints bc; these stresses are often formed by the counterclockwise rotation of the Arabian Plate, in addition to the local forces. Three types of faults, thrust, backthrust, and dextral movement, strongly affected the structural model of the fold, causing the vergence to change between the rocks of different formations along the traverse. After the Pilaspi Formation (Late Eocene) was deposited, the pre-existing normal or listric fault, mentioned above, was reactivated with positive inversion, making the southwestern limb steeper than the northeastern limb within rocks of the Pilaspi Formation. This fault was accompanied by strike-slip movement that affected the area, forming distinct structures on both sides. A period of relaxation occurred, during which normal faults and tension joints formed. Following the deposition of the Fatha Formation (Middle Miocene) and Injana Formation (Late Miocene), the detachment fault was reactivated. Still, its impact on the rocks of the two formations at the northeast limb was steeper than in the southwest limb, where the fault behaved as a backthrust. A second relaxation stage began after the back thrust stage.

Conflict of interest: The authors declared no conflicts of interest.

Sources of funding: This research did not receive any specific grant from funding agencies in the public, commercial, or not-for-profit sectors.

Author contributions: The authors contributed equally to the study.

REFERENCES

1. Bonham-Carter G, Qiuming C. Progress in geomathematics: Springer Science & Business Media; 2008.

2. Dunne W, Hancock P, editors. Palaeostress analysis of small-scale brittle structures. Continental deformation; 1994.

3. Davis GH, Reynolds SJ, Kluth CF. Structural geology of rocks and regions: John Wiley & Sons, 2011.

4. Belayneh M. Palaeostress orientation inferred from surface morphology of joints on the southern margin of the Bristol Channel Basin, UK. 2004. https://doi.org/10.1144/GSL.SP.2004.231.01.14

5. Smeraglia L, Fabbi S, Cipriani A, Consorti L, Sirna M, Corbi F, et al. Deformation mechanisms and slip behaviors of tectonically deformed conglomerates from the Central Apennines fold-and-thrust belt: Implications for shallow aseismic and seismic slip. Journal of Structural Geology. 2024;186:105202. https://doi.org/10.1016/j.jsg.2024.105202

6. Numan NM. A plate tectonic scenario for the Phanerozoic succession in Iraq. Iraqi Geological Journal. 1997;30(2):85-110.

7. Numan NM. Cretaceous and Tertiary Alpine subductional history in northern Iraq. Iraqi Journal of Earth Science. 2001;1(2):59-74. https://doi.org/10.1016/S0191-8141(01)00075-X

8. Mohajjel M, Fergusson CL. Dextral transpression in Late Cretaceous continental collision, Sanandaj–Sirjan zone, western Iran. Journal of Structural Geology. 2000;22(8):1125-39.

9. Aghazadeh M, Castro A, Badrzadeh Z, Vogt K. Post-collisional polycyclic plutonism from the Zagros hinterland: the Shaivar Dagh plutonic complex, Alborz belt, Iran. Geological Magazine. 2011;148(5-6):980-1008.

10. Alipour M. Collision along irregular plate margin controlled the tectono-stratigraphic evolution of the Iranian Zagros fold and thrust belt. Marine and Petroleum Geology. 2023;154:106311. https://doi.org/10.1016/j.marpetgeo.2023.106311

11. Namdarsehat P, Milczarek W, Bugajska-Jędraszek N, Motavalli-Anbaran S-H, Khaledzadeh M. Uncovering a Seismogenic Fault in Southern Iran through Co-Seismic Deformation of the Mw 6.1 Doublet Earthquake of 14 November 2021. Remote Sensing. 2024;16(13):2318. https://doi.org/10.3390/rs16132318

12. Ayyed Hussein W, Thair Mudhir F, Hasnaa Saleh K. Variation of the Anticlines Vergency in the Iraqi Zagros Folds Belt and Its Tectonic Indications. Tikrit Journal of Pure Science. 2020;25(2):64-70. https://doi.org/10.25130/tjps.v25i2.237

13. Al-Jawadi AS, Bety AKS, Ismaeel OA. Lineament analysis using remote sensing and GIS techniques in the Sangaw Area, Kurdistan Region, NE Iraq. The Iraqi Geological Journal. 2022:152-63. https://doi.org/10.46717/igj.55.2C.11ms-2022-08-24

14. Sembroni A, Reitano R, Faccenna C, Callieri P. The geologic configuration of the Zagros Fold and Thrust Belt: an overview. Mediterranean Geoscience Reviews. 2024;6(2):61-86. https://doi.org/10.1007/s42990-024-00118-6

15. Numan N, Azzawi N. Structural and geotectonic interpretation of vergence directions of anticlines in the foreland folds of Iraq. 1993.

16. Sissakian VK, Al-Jiburi BS. Stratigraphy of the high folded zone. Iraqi Bulletin of Geology and Mining. 2014(6):73-161.

17. Bellen RV, Dunnington H, Wetzel R, Morton D. Lexique stratigraphique international Asie. Iraq Intern Geol Conger Comm Stratigr. 1959;3:333.

18. Hancock P. Brittle microtectonics: principles and practice. Journal of structural geology. 1985;7(3-4):437-57. https://doi.org/10.1016/0191-8141(85)90048-3